A colorimetric nitrite detection system with excellent selectivity and high sensitivity based on Ag@Au nanoparticles†

Tianhua Li,‡[a,b] Yonglong Li,‡[a,c] Yujie Zhang,[a] Chen Dong,[a] Zheyu Shen*[a] and Aiguo Wu*[a]

Excessive uptake of NO_2^- is detrimental to human health, but the currently available methods used to sensitively detect this ion in the environment are cumbersome and expensive. In this study, we developed an improved NO_2^- detection system based on a redox etching strategy of CTAB-stabilized Ag–Au core–shell nanoparticles (Ag@AuNPs). The detection mechanism was verified by UV-Vis spectroscopy, TEM and XPS. The detection system produces a color change from purple to colorless in response to an increase of NO_2^- concentration. The selectivity of detection of NO_2^-, both with the unaided eye and by measurement of UV-Vis spectra, is excellent in relation to other ions, including Cu^{2+}, Co^{2+}, Ni^{2+}, Cr^{3+}, Al^{3+}, Pb^{2+}, Cd^{2+}, Ca^{2+}, Ba^{2+}, Zn^{2+}, Mn^{2+}, Mg^{2+}, Fe^{3+}, Hg^{2+}, Ag^+, K^+, F^-, PO_4^{3-}, $C_2O_4^{2-}$, SO_3^{2-}, CO_3^{2-}, SO_4^{2-}, NO_3^- and $CH_3–COO^-$ (Ac^-). The limit of detection (LOD) for NO_2^- is 1.0 μM by eye and 0.1 μM by UV-Vis spectroscopy. The LOD by eye is lower than the lowest previously reported value (4.0 μM). There is a good linear relationship between A/A_0 and the concentration of NO_2^- from 1.0 to 20.0 μM NO_2^-, which permits a quantitative assay. The applicability of our detection system was also verified by analysis of NO_2^- in tap water and lake water. The results demonstrate that our Ag@AuNP-based detection system can be used for the rapid colorimetric detection of NO_2^- in complex environmental samples, with excellent selectivity and high sensitivity.

1. Introduction

Nitrite ion (NO_2^-) is an essential inorganic nitrogen-containing nutrient used, alongside NH_4^+ and NO_3^-, in fertilizers to promote the growth of plants.[1,2] It is also widely used in the food preservation industries. However, excessive uptake of NO_2^- is detrimental to human health and may cause stomach cancer; moreover, NO_2^- reacts with amines, resulting in the formation of nitroso compounds, and it reacts with oxyhemoglobin to produce methemoglobin irreversibly in the blood stream, thereby interfering with oxygen transport in the blood and causing methemoglobinemia.[3–5] It is of great importance to determine the concentration of NO_2^- in food, the environment, urine and other biological samples. Much effort has been devoted to such NO_2^- detection, including by the use of fluorophores,[5,6] ion chromatography[7,8] and electrochemistry.[9–12] Their limits of detection (LODs) are lower than the NO_2^- toxicity level (1 ppm, 21.7 μM), which is defined for drinking water by the U.S. Environmental Protection Agency (US EPA).[13] However, the existing analytical methods referred to above usually require expensive equipments, and the sample preparation processes are complicated, time-consuming and unsuitable for on-site analysis. Therefore, the development of a facile and inexpensive analytical method for detecting NO_2^- is urgently demanded.

Fluorescent and colorimetric sensors have aroused widespread interest during the past two decades.[5,14–17] Gold nanoparticles (AuNPs), which possess a high molar extinction coefficient and high stability, have been extensively applied in colorimetric assays for the detection of NO_2^- in food or waste water.[16–19] For example, Mirkin *et al.* designed two kinds of functionalized AuNPs to detect NO_2^-, in a method based on the Griess reaction.[18] Xiao *et al.* reported a non-crosslinking colorimetric NO_2^- sensor with an LOD for NO_2^- of 20 μM

[a]*Key Laboratory of Magnetic Materials and Devices, & Division of Functional Materials and Nano Devices, Ningbo Institute of Materials Technology & Engineering, Chinese Academy of Sciences, Ningbo, Zhejiang 315201, China. E-mail: aiguo@nimte.ac.cn, shenzheyu@nimte.ac.cn; Fax: +86 574 86685163; Tel: +86 574 86685039*

[b]*Faculty of Materials Science and Chemical Engineering, Ningbo University, Ningbo 315211, China*

[c]*Nano Science and Technology Institute, University of Science and Technology of China, Suzhou, Jiangsu 215123, China*

based on a deamination reaction induced by NO_2^-, which resulted in aggregation of the gold nanorods.[19] However, these colorimetric sensors need modification of the AuNP surface with specific ligands. After the development of these sensors, Zhang *et al.* developed a colorimetric NO_2^- sensor using unmodified AuNPs, based on a specific diazo reaction between NO_2^- and phenylenediamine.[20] This method is not practical because the detection process is complicated and the detection range is not broad. Chen *et al.* developed a colorimetric method for NO_2^- detection based on etching of gold nanorods (AuNRs), which uses a new redox reaction detection strategy rather than the diazo reaction. The LOD for NO_2^- by the naked eye using this method, at 4.0 μM,[21] is lower than that using any other reported method. However, heating is necessary for the detection in this case, and an interfering ion (Fe^{3+}) may also limit the application of the method in naturally occurring samples.

In this study, we developed an improved system based on a redox etching strategy of CTAB-stabilized Ag–Au core–shell nanoparticles (Ag@AuNPs) for NO_2^- detection without heating. This system has a higher sensitivity (the LOD to the naked eye is 1.0 μM) and better selectivity (no interfering ion exists) than the previously reported methods.

2. Experimental section

2.1 Materials and apparatus

Sodium nitrite ($NaNO_2$), magnesium chloride ($MgCl_2$), sodium nitrate ($NaNO_3$) and sodium fluoride (NaF) were purchased from Aladdin Reagent Co., Ltd (Shanghai, China). Silver nitrate ($AgNO_3$), trisodium citrate dehydrate ($C_6H_5Na_3O_7{\cdot}2H_2O$), sodium borohydride ($NaBH_4$), chloroauric acid ($HAuCl_4$), cetyltrimethyl ammonium bromide (CTAB), hydroxylamine hydrochloride ($NH_2OH{\cdot}HCl$) and other essential reagents were obtained from Sinopharm Chemical Reagent Co., Ltd (Beijing, China). All reagents were used as received without further purification. Glassware was washed using aqua regia ($HCl–HNO_3$ = 3 : 1 (v/v)), and then cleaned with Milli-Q water.

Surface plasmon resonance (SPR) absorption data were recorded with an ultraviolet and visible spectrophotometer (UV-Vis, PERSEE T10CS). Transmission electron microscopy (TEM) images were acquired using a JEOL 2100 microscope operating at an accelerating voltage of 200 KV. X-ray photon spectrometry (XPS) was performed using an AXIS Ultra DLD instrument with Mg Kα radiation as the X-ray source.

2.2 Synthesis of Ag@AuNPs

Ag@AuNPs were synthesized according to the reported method, with modifications.[24] Typically, aqueous solutions of $AgNO_3$ (20 mM, 2.0 mL) and $C_6H_5Na_3O_7{\cdot}2H_2O$ (30 mM, 6.0 mL) were mixed with 174 mL of Milli-Q water in a 300 mL beaker and stirred vigorously at room temperature. Then, 2.0 mL of fresh $NaBH_4$ aqueous solution (100 mM) was added dropwise to the above mixture, with stirring. The reaction was kept for 2.0 h at room temperature (the color of the solution became pale yellow). Aqueous solutions of $NH_2OH{\cdot}HCl$ (62.5 mM, 10 mL) and $HAuCl_4$ (5.0 mM, 10 mL) were then simultaneously added (2.0 mL min^{-1}) into the above system. The obtained mixture was stirred for another 45 min (during which time the color of the solution changed from light yellow to crimson). The obtained Ag@AuNP solutions were centrifuged at 15 000*g* for 15 min and then resuspended in 100 mL of various concentrations of aqueous CTAB (from 5.0 to 100 mM).

2.3 Sensing detection of NO_2^-

The colorimetric detection of NO_2^- was carried out at room temperature. First, the pH values of the prepared dispersions of Ag@AuNPs were respectively adjusted to 1.0–1.5. Then, 100 μL of different concentrations of NO_2^- were respectively added into 900 μL of the Ag@AuNP dispersions, and the mixtures were shaken and stored at ambient conditions for 1.0–30 min. Finally, the change in color and the corresponding UV-Vis absorption spectra were recorded.

2.4 Selective detection of NO_2^-

To verify the selectivity of our proposed detection system based on Ag@AuNPs, other ions including Cu^{2+}, Co^{2+}, Ni^{2+}, Cr^{3+}, Al^{3+}, Pb^{2+}, Cd^{2+}, Ca^{2+}, Ba^{2+}, Zn^{2+}, Mn^{2+}, Mg^{2+}, Fe^{3+}, Hg^{2+}, Ag^+, K^+, F^-, PO_4^{3-}, $C_2O_4^{2-}$, SO_3^{2-}, CO_3^{2-}, SO_4^{2-}, NO_3^- and Ac^- were also tested in a similar manner to that mentioned above. The concentration of each of the ions used in determining selectivity was 200 μM, except for NO_2^-, Fe^{3+} and Cu^{2+}, for which the concentration was 20 μM.

2.5 Detection of NO_2^- in commonly available sources of water

Samples of tap water obtained from our institution and lake water collected from a pond in our institution were filtered through a 0.2 μm membrane, and then spiked with standard NO_2^- stock solutions of various concentrations. The NO_2^- was then detected using colorimetry and UV-Vis spectroscopy as mentioned above.

3. Results and discussion

3.1 Sensing strategy

The design of our Ag@AuNP-based system for NO_2^- detection is shown in Scheme 1. The standard redox potentials of $AuBr_2^-$/Au and $AuBr_4^-$/Au are 0.85 V and 0.93 V, respectively. However, the actual redox potential of HNO_2/NO is approximately 1.0 V for a pH of 1.3, which enables NO_2^- to oxidize AuNPs to form $AuBr_2^-$ or $AuBr_4^-$ in the presence of CTAB. Moreover, it was reported that CTAB could be used to reduce the redox potentials of $AuBr_2^-$/Au or $AuCl_2^-$/Au to less than 0.4 V due to the formation of $AuBr_2^-$–CTA^+ complex.[22] Therefore, the redox etching of our CTAB-stabilized Ag@AuNPs is easily induced by NO_2^-. We chose Ag@AuNPs rather than AuNRs because the Ag@AuNPs prepared by the galvanic reaction between gold and silver[23] can increase the color response when NO_2^- is detected. Here, NO_2^- could be directly detected

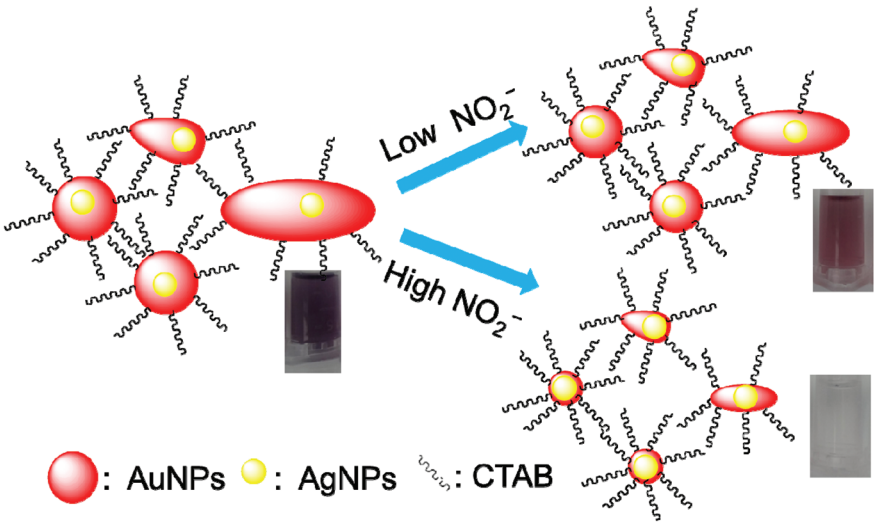

Scheme 1 Schematic illustration of the etching mechanism based on Ag@AuNPs.

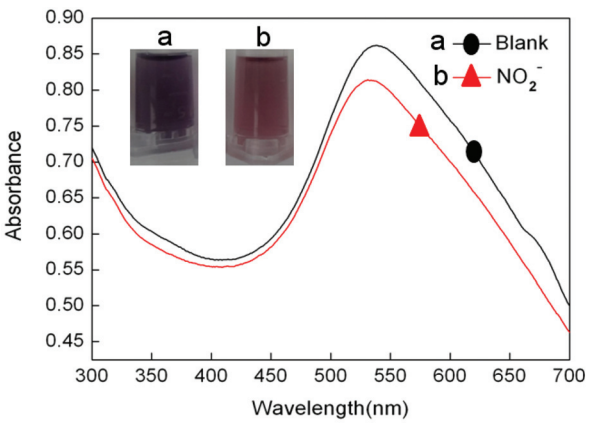

Fig. 1 UV-Vis spectra of the Ag@AuNP dispersions in the presence of CTAB (100 mM) without NO_2^- (a) or Ag@AuNP dispersions incubated with 10.0 μM NO_2^- (b) for 15 min. The inset image corresponds to the colorimetric response. The pH value of the Ag@AuNP dispersions was maintained at 1.3.

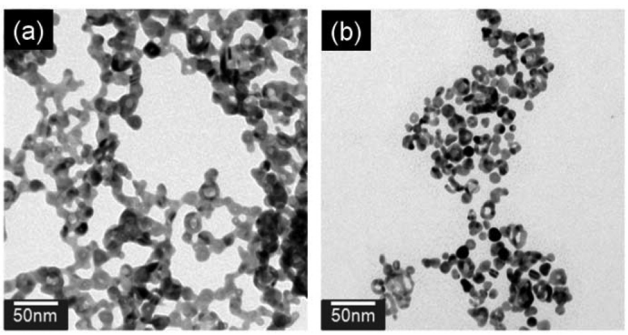

Fig. 2 TEM images of the Ag@AuNPs without NO_2^- incubation (a) and the Ag@AuNPs incubated with (b) 10.0 μM NO_2^-.

by visualizing the color change of the Ag@AuNP dispersion using the naked eye, with high sensitivity and excellent selectivity.

This mechanism for detecting NO_2^-, *i.e.*, redox etching of Ag@AuNPs (Scheme 1), was verified by UV-Vis spectroscopy, TEM and XPS. Fig. 1 shows the UV-Vis spectra and photographic images of the Ag@AuNP dispersions in the presence of CTAB (100 mM) with or without incubation with NO_2^-. The pH value of the Ag@AuNP dispersions was controlled to be 1.3. The Ag@AuNP dispersion was purple in color and had a UV-Vis absorption spectrum with a peak wavelength at 536 nm. After being incubated with 10 μM of NO_2^- for 15 min, the Ag@AuNP dispersion changed in color from purple to red. In addition, the peak wavelength shifted to 526 nm. The blue shift of the absorption peak may be attributed to the decrease of the nanoparticle sizes.[21,25]

Fig. 2 shows the corresponding TEM images of the Ag@AuNPs with or without incubation with NO_2^-. Due to the galvanic reaction between gold and silver, the prepared Ag@AuNPs aggregated (Fig. 2a). After being incubated with 10 μM of NO_2^- for 15 min, the Ag@AuNPs became well dispersed, and the particle size decreased (Fig. 2b). This result indicates that the Ag@AuNPs were etched by NO_2^- under acidic conditions.

To further verify the etching mechanism, XPS was used to characterize the binding energy of Au 4f, as shown in Fig. 3. Compared with the Au 4f XPS spectrum of Ag@AuNPs without NO_2^-, that of the Ag@AuNPs incubated with 10 μM of NO_2^- displayed an obvious shift, indicating that the chemical environment changed as a result of the leaching of the surface Au atoms.

These results verify the above-mentioned mechanism for NO_2^- detection, *i.e.*, NO_2^- can easily etch the Ag@AuNPs.

3.2 Optimization of the experimental conditions

The pH value of the Ag@AuNPs, the concentration of CTAB in the Ag@AuNPs and the incubation time of Ag@AuNPs and

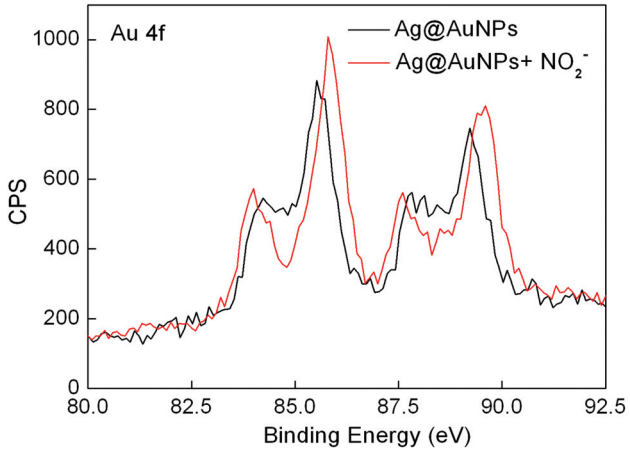

Fig. 3 Au 4f of XPS spectra of the Ag@AuNPs without NO_2^- incubation (a) and of the Ag@AuNPs incubated with 10.0 μM NO_2^- (b).

NO_2^- were optimized according to the sensing effect of our Ag@AuNP-based detection system for NO_2^-.

The redox reaction rate of AuNRs increases with decreasing pH.[21] However, the Ag@AuNP system is not stable when the pH value is lower than 1.0. Moreover, Fe^{3+} and Cu^{2+} can interfere with the NO_2^- detection at pH 1.0 because they can also oxidize the Ag@AuNPs nanoparticles at pH 1.0 resulting in a color change (Fig. S1†). Therefore, the pH value was fixed at 1.3 for the subsequent experiments.

The color of the Ag@AuNP dispersions in the presence of NO_2^- changed stepwise from purple to red when the concentration of CTAB was increased from 5.0 to 100 mM (Fig. S2a†). The color change (Fig. S2a†) and the decrease of A/A_0 (Fig. S2b†) with increasing CTAB concentration provided two supporting pieces of evidence confirming that the chemical etching process could be accelerated by CTAB, which reduces the electron potential of $AuBr_2^-$/Au or $AuCl_2^-$/Au to less than 0.4 V.[22] Considering the solubility of CTAB, its optimal concentration is fixed at 100 mM in the following study.

Furthermore, the incubation time for Ag@AuNPs and NO_2^- was also optimized. The value of A/A_0 was plotted as a function of the incubation time (Fig. S3†) (A: the absorbance value at 526 nm in the UV-Vis spectra of the Ag@AuNP-based detection systems incubated with NO_2^-; A_0: the absorbance value at 536 nm in the UV-Vis spectra of Ag@AuNP-based detection systems without NO_2^- incubation). Because the value of A/A_0 was observed to decrease significantly within 15 min and then to remain constant thereafter, the incubation time was fixed at 15 min as an optimized value for the subsequent study.

3.3 Selectivity of the NO_2^- detection system

The selectivity of our proposed Ag@AuNP-based detection system for NO_2^- was evaluated with the unaided eye and UV-Vis spectra by comparing the results with those obtained with samples containing other ions, including Cu^{2+}, Co^{2+}, Ni^{2+}, Cr^{3+}, Al^{3+}, Pb^{2+}, Cd^{2+}, Ca^{2+}, Ba^{2+}, Zn^{2+}, Mn^{2+}, Mg^{2+}, Fe^{3+}, Hg^{2+}, Ag^+, K^+, F^-, PO_4^{3-}, $C_2O_4^{2-}$, SO_3^{2-}, CO_3^{2-}, SO_4^{2-}, NO_3^- and Ac^-. Fig. 4a shows a photograph of the Ag@AuNP-based detection systems incubated with NO_2^- in the presence of Fe^{3+}, Cu^{2+} or other ions. Only the sample with NO_2^- changed from purple to red. As shown in Fig. 4b, NO_2^- is also the only ion whose absorption peak shifted from 536 nm to 526 nm with an evident decrease of the absorption intensity. These results indicate that the Ag@AuNP etching process can only be induced by NO_2^-.

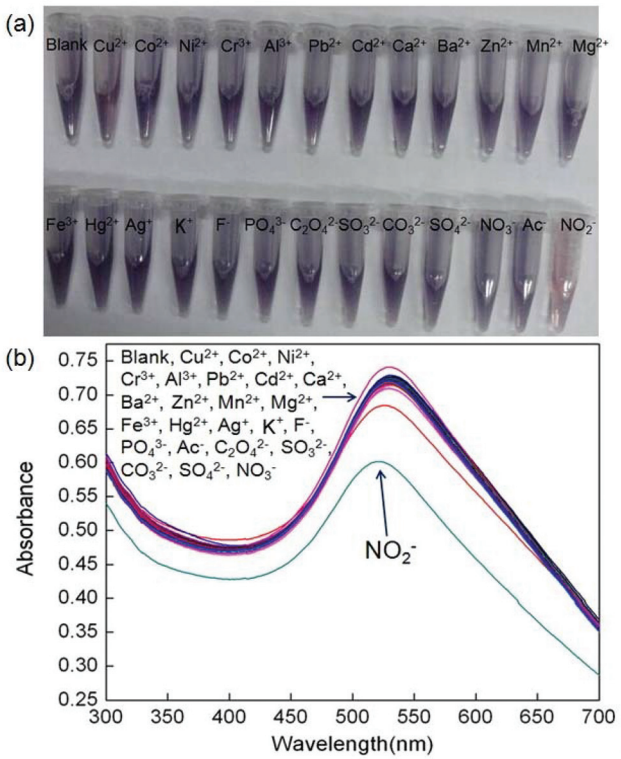

Fig. 4 Selectivity of the Ag@AuNP-based detection system for NO_2^- compared with other ions. (a) Photograph of the detection systems incubated with NO_2^- (20 μM), Fe^{3+} (20 μM), Cu^{2+} (20 μM) or other ions (200 μM); (b) UV-Vis absorption spectra of the detection systems incubated with NO_2^- (20 μM), Fe^{3+} (20 μM), Cu^{2+} (20 μM) or other ions (200 μM).

The selectivity of the Ag@AuNP-based detection system for NO_2^- was also verified by investigating the influence of various other ions on the NO_2^--sensing effect. The color of the Ag@AuNP-based detection systems incubated with both NO_2^- (20 μM) and other single ions (20 μM) changed from purple to red, which is very similar to that produced in the absence of any other single ion (Fig. S4a†). The UV-Vis absorption spectra of the detection systems incubated with 20 μM of NO_2^- and 20 μM of other single ions shifted from 536 nm to 526 nm with an obvious decrease of the absorption intensity. These results are very similar to those of the detection system incubated with NO_2^- alone (Fig. S4b†), and thus demonstrate that these various other ions have no influence on the NO_2^- sensing effect of our Ag@AuNP-based detection system. This detection system for NO_2^- clearly exhibits excellent selectivity.

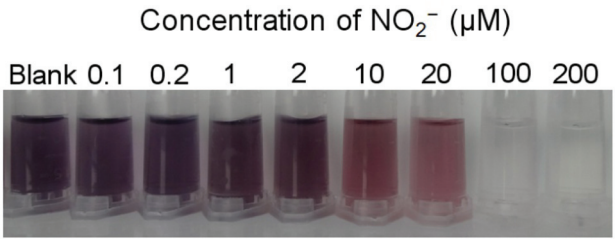

Fig. 5 Photographic image of the Ag@AuNP-based detection system incubated with various concentrations of NO_2^- ranging from 0 to 200 μM.

3.4 Sensitivity of the NO_2^- detection system

The colorimetric response and UV-Vis absorption spectra were used to evaluate the sensitivity of our Ag@AuNP-based NO_2^- detection system. Fig. 5 shows colorimetric images of this detection system after incubation with various concentrations of NO_2^- from 0.1 to 200 μM. The detection systems changed from purple to colorless with increasing concentration of NO_2^-, with a limit of detection (LOD) to the naked eye of 1.0 μM, which is lower than the previously-reported value of 4.0 μM.[21] Furthermore, compared with the reported AuNR-based detection system,[21] our Ag@AuNP-based detection system has two additional advantages: the detection process is simpler and is fast, without requiring heating, whereas heating is necessary for the previously-reported AuNR-based detection system; and the selectivity is excellent and lacks interference from other ions, whereas interference from Fe^{3+} doers occur for the previously-reported AuNR-based detection system.

Fig. 6a shows the UV-Vis absorption spectra of the Ag@AuNP-based detection systems incubated with various concentrations of NO_2^-. As the concentration of NO_2^- was increased from 0 to 100 μM, the UV-Vis absorption spectrum exhibited a blue-shift with a decrease of the absorption intensity due to the change in the morphology of the Ag@AuNPs induced by NO_2^-. The LOD of our NO_2^- detection system was observed to be 0.1 μM by UV-Vis spectroscopy, which is comparable to that of the AuNR-based detection system.[21] The UV absorbance peak at 400 nm for AgNPs[26] did not appear when the NO_2^- concentration was increased (Fig. 6a). This may be because the Au shell was thickly and uniformly coated around the Ag core and could not have been etched thoroughly at the 100 μM maximum NO_2^- concentration of this study.

Fig. 6b shows a good linear relationship (R^2 = 0.9911) between A/A_0 and NO_2^- concentration in the range from 1.0 to 20.0 μM (A: the absorbance value at 526 nm in the UV-Vis spectra of Ag@AuNP-based detection systems incubated with NO_2^-; A_0: the absorbance value at 536 nm in the UV-Vis spectra of Ag@AuNP-based detection systems without NO_2^- incubation). This relationship indicates that our detection system may be applied to the quantitative assay of NO_2^-.

Taken together, these results indicate that our Ag@AuNP-based detection system is applicable for rapid colorimetric detection of NO_2^-, with excellent selectivity and high sensitivity.

3.5 Analysis of common water samples

To confirm that our NO_2^- detection system could be used in practice, it was used to analyze tap water and lake water. As shown in Table 1, the amount of NO_2^- added to each of these water samples was very similar to the amount detected (by our detection system using UV-Vis spectroscopy), which indicates the feasibility and sensitivity of our NO_2^- detection system. These results reinforce our proposal that this detection system can be used for the analysis of NO_2^- in environmental samples.

4. Conclusions

In this study, we developed an improved NO_2^- detection system based on a redox etching strategy using CTAB-stabilized Ag@AuNPs. The detection mechanism was verified by using UV-Vis spectroscopy, TEM and XPS. According to the sensing

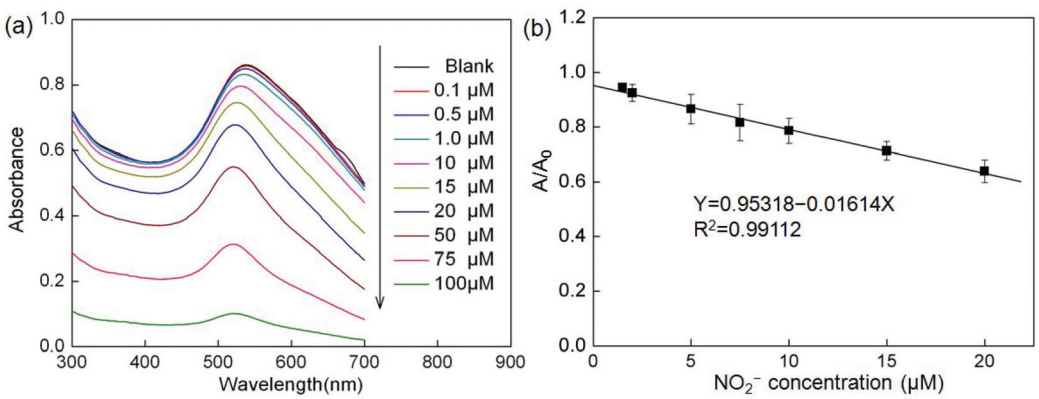

Fig. 6 (a) UV-Vis absorption spectra of the Ag@AuNP-based detection systems incubated with various concentrations of NO_2^-. (b) Plot of A/A_0 *versus* NO_2^- concentration in the range of 1.0–20.0 μM (mean ± SD, n = 3). A: the absorbance value at 526 nm in the UV-Vis spectra of Ag@AuNP-based detection systems incubated with NO_2^-; A_0: the absorbance value at 536 nm in the UV-Vis spectra of Ag@AuNP-based detection systems without incubation with NO_2^-.

Table 1 Determination of NO_2^- in water samples (n = 3)

Sample	Added[a] (μM)	Detected[b] (μM) (mean ± SD)	Recovery[c] (%)
Tap water	5.0	5.41 ± 0.12	108.2
	10.0	8.96 ± 0.24	89.6
Lake water	5.0	4.23 ± 0.18	84.6
	10.0	7.56 ± 0.11	75.6

[a] Amount of NO_2^- added to samples of commonly-occurring sources of water. [b] NO_2^- concentration in these water samples determined by our detection system using UV-Vis spectroscopy. [c] Calculated from the equation: (detected value with NO_2^- addition – detected value without NO_2^- addition)/added value.

effect, the CTAB concentration, NO_2^- incubation time and pH value of the detection system were optimized to be 100 mM, 15 min and 1.3, respectively. Under the optimized conditions, the ability of our system to selectively detect NO_2^-, whether with the unaided eye or using UV-Vis spectroscopy, is excellent compared to the ability to similarly detect other ions. In addition, our Ag@AuNP-based detection system is highly sensitive for NO_2^-, whose LOD is 1.0 μM by eye and 0.1 μM by UV-Vis spectroscopy. A highly linear relationship (R^2 = 0.9911) was observed between A/A_0 and NO_2^-, from 1.0 μM to 20.0 μM NO_2^-, which can be used for a quantitative assaying of NO_2^-. This detection system also exhibits satisfactory performance using samples of water from commonly-occurring sources. Consequently, these results reinforce the applicability of our Ag@AuNP-based detection system for the rapid colorimetric detection of NO_2^- in complicated environmental samples.

Acknowledgements

This work was supported by the Program of Zhejiang Provincial Natural Science Foundation of China (R5110230, LQ13E030004), the National Natural Science Foundation of China (31128007, 51203175), the Hundred Talents Program (2010-735) and the STS program (KFJ-EW-STS-016) of the Chinese Academy of Sciences, the aided program of the Science and Technology Innovative Research Team of Ningbo Municipality (2014B82010), and the Zhejiang Postdoctoral Maintenance Fund (Bsh1201009).

Notes and references

1 M. J. Hill, *Nitrates and Nitrites in food and water*, Woodhead Publishing Limited, England, 1st edn, 1996.
2 J. C. Fanning, *Coord. Chem. Rev.*, 2000, **199**, 159–179.
3 R. Walker, *Food Addit. Contam., Part A*, 1990, **7**, 717–768.
4 S. A. Kyrtopoulos, *Cancer Surv.*, 1989, **8**, 423–442.
5 B. Unnikrishnan, S. C. Wei, W. J. Chiu, J. S. Cang, P. H. Hsu and C. C. Huang, *Analyst*, 2014, **139**, 2221–2228.
6 L. J. Dombrowski and E. J. Pratt, *Anal. Chem.*, 1972, **44**, 2268–2272.
7 J. M. Doyle, M. L. Miller, B. R. McCord, D. A. McCollam and G. W. Mushrush, *Anal. Chem.*, 2000, **72**, 2302–2307.
8 S. Rokushika, F. M. Yamamoto and K. Kihara, *J. Chromatogr.*, 1993, **630**, 195–200.
9 G. Yildiz, N. Oztekin, A. Orbay and F. Senkal, *Food Chem.*, 2014, **152**, 245–250.
10 Y. H. Cheng, C. W. Kung, L. Y. Chou, R. Vittal and K. C. Ho, *Sens. Actuators, B*, 2014, **192**, 762–768.
11 J. J. Jiang, W. J. Fan and X. Z. Du, *Biosens. Bioelectron.*, 2014, **51**, 343–348.
12 Y. Wang, E. Laborda and R. G. Compton, *J. Electroanal. Chem.*, 2012, **670**, 56–61.
13 United States Environmental Protection Agency, *National Primary Drinking Water Regulations: Contaminant Specific Fact Sheets*, Inorganic Chemicals, Consumer Version, Washington, DC, 2009.
14 Z. Wang and L. Ma, *Coord. Chem. Rev.*, 2009, **253**, 1607–1618.
15 Y. Song, W. Wei and X. Qu, *Adv. Mater.*, 2011, **23**, 4215–4236.
16 R. Wang, F. B. Yu, P. Liu and L. X. Chen, *Chem. Commun.*, 2012, **48**, 5310–5312.
17 Z. Y. Zhang, Z. P. Chen, S. S. Wang, C. L. Qu and L. X. Chen, *ACS Appl. Mater. Interfaces*, 2014, **6**, 6300–6307.
18 W. L. Daniel, M. S. Han, J. S. Lee and C. A. Mirkin, *J. Am. Chem. Soc.*, 2009, **131**, 6362–6363.
19 N. Xiao and C. X. Yu, *Anal. Chem.*, 2010, **82**, 3659–3663.
20 J. Zhang, C. Yang, X. L. Wang and X. R. Yang, *Analyst*, 2012, **137**, 3286–3292.
21 Z. P. Chen, Z. Y. Zhang, C. L. Qu, D. W. Pan and L. X. Chen, *Analyst*, 2012, **137**, 5197–5200.
22 J. Rodriguez-Fernandez, J. Perez-Juste, P. Mulvaney and L. M. Liz-Marzan, *J. Phys. Chem. B*, 2005, **109**, 14257–14261.
23 X. M. Lu, H. Y. Tuan, J. Y. Chen, Z. Y. Li, B. A. Korgel and Y. N. Xia, *J. Am. Chem. Soc.*, 2007, **129**, 1733–1742.
24 I. Srnova-Sloufova, F. Lednicky, A. Gemperle and J. Gemperlova, *Langmuir*, 2000, **16**, 9928–9935.
25 R. X. Zou, X. Guo, J. Yang, D. D. Li, F. Peng, L. Zhang, H. J. Wang and H. Yu, *CrystEngComm*, 2009, **11**, 2797–2803.
26 L. J. Miao, J. W. Xin, Z. Y. Shen, Y. J. Zhang, H. Y. Wang and A. G. Wu, *Sens. Actuators, B*, 2013, **176**, 906–912.